

# Modeling Hot Carriers Quantum Well Solar Cells

Hamid Fardi

**Abstract**— The effects of carrier escape from quantum well (*QW*) and the interaction of hot electrons with crystal lattice are of importance to the physical understanding of *QW* hot carrier solar cells when the cooling dynamics in photo-excited structures affect the cell efficiency. The absorption of high-energy photons produces electron hole pairs with excess kinetic energy, which are dissipated to the lattice thru phonon scattering. These hot electrons alter the conversion efficiency in photovoltaic solar cells. We have studied hot electron effects in an  $Al_xGa_{1-x}As$  /  $GaAs$  p-i-n structure with quantum wells are placed in the intrinsic region similar to the experimental device structure reported by others. Our results show that hot electrons lead to an increase in short circuit current. The increase in short circuit current is due to carriers escaping from the well without any significant recombination loss which leads to a higher cell efficiency. These results support the experimental data recently published by others.

**Index Terms**— Hot carriers, quantum wells, solar cells

## I. INTRODUCTION

It is important to model devices with the precise engineering of the band gaps to optimize the absorption incorporating quantum well layers into one or more of the subcells, allowing some leverage to design and fabricate devices for the absorption threshold to match the current generated in each subcell due to local absorption of the sun spectrum.

Single crystal quantum well solar cells are considered devices with high efficiency energy conversion used for application in both single and

multijunction photovoltaic cells, as their capability outperform bulk devices under concentrated illumination close to the single gap

Shockley-Queisser limit for the same bulk materials[1].

In order to further increase the efficiency, the mechanisms behind the extraordinary performance need to be analyzed and understood. This paper present a model for the device behavior based on complex processes between localized and extended states, such as carrier capture and escape into and from quantum wells, which is described by the combination of macroscopic semiconductor transport equations and detailed balance rate equations.

The effects of carrier escape from *QW* and the interaction of hot electrons with crystal lattice are of importance to the physical understanding of *QW* hot carrier solar cells where the cooling dynamics in photo-excited structures affect the cell efficiency. The absorption of high-energy photons produces electron hole pairs with excess kinetic energy, which are dissipated to the lattice thru phonon scattering. Quantum wells were proposed as one approach in utilizing these carriers with excess kinetic energy. These hot electrons, so called hot carriers, alter the conversion efficiency in photovoltaic solar cells.

A microscopic numerical approach based on the non-equilibrium *Green's* function that takes into the consideration the interaction of quantum optics and dissipative quantum energy levels is used to model the quantum kinetic levels in photovoltaic's as it is discussed in [2-7]. Their modeling approach is capable of analyzing devices at reduced size and

H. Fardi is with the Department of Electrical Engineering, University of Colorado Denver, Denver, CO 80217 USA (hamid.fardi@ucdenver.edu). National Institute of Standards and Technology, Boulder, CO 80305 USA (corresponding author to provide phone: 303-555-5555; fax: 303-555-5555; e-mail: author@boulder.nist.gov).

dimensionality with a high computation time limitations.

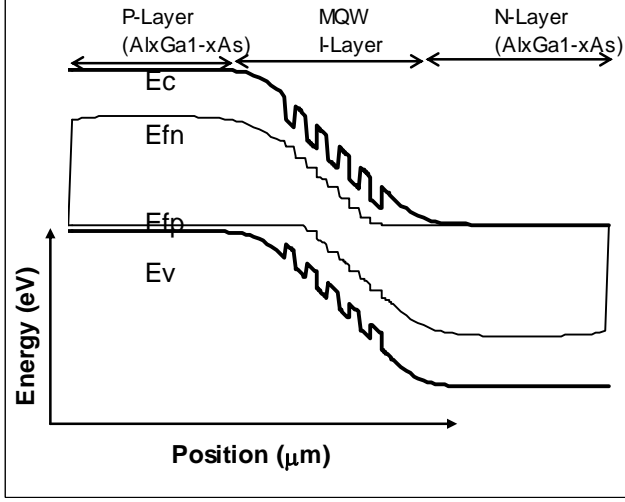


Figure 1. Band structure of a multi quantum well  $\text{Al}_x\text{Ga}_{1-x}\text{As} / \text{GaAs}$  cell. The wells are treated as single QW's with no overlap and coupling effect.

Our approach to device modeling for studying hot electrons in quantum well has been approximated by the numerical solution of the energy balance equations coupled with non-isothermal drift diffusion transport equations. The size quantization and the two-dimensional (2D) density of states are applied in the quantum wells. The assumptions made are: (a) quasi Fermi level is flat in the well, shown for the structure modeled in Figure 1, (b) the transition between 2D density of states and the bulk states (for calculating free carrier concentration) is abrupt, (c) in the QW, *Boltzmann* statistics describes the free and bound carrier concentrations, however the bound charge is dependent on the quantum well thickness, 2D density of states, and quantized energy level and wave-function, (d) a finite square well solution to wave function is used for the energy levels. The wells are treated as single QW's with no overlap and coupling effect. Various generation-recombination mechanisms are included, that is; electron-hole generation due to optical absorption, generation-recombination due to *Shockley-Read-Hall* (SRH), and band-to-band radiative mechanisms. Energy transfer among the charge carriers and crystal lattice is modeled by an energy relaxation lifetime.

## II. DEVICE MODELING

The carrier rate equations, Poisson's equation, and auxiliary drift-diffusion current equations are solved coupled with the energy-balance equations to compute the internal electron temperature. The conventional drift-diffusion equations as well as Poisson equation are solved to describe the device current-voltage characteristics in the bulk region of the semiconductor, and outside the quantum wells. The device formulation follows. The Poisson equation:

$$\varepsilon_s \nabla^2 \cdot \psi(x) - q[p(x) - n(x) + N_D(x) - N_A(x)] = 0 \quad (1)$$

where  $N_D(x)$  and  $N_A(x)$  are position dependent donor and acceptor densities;  $n(x)$  and  $p(x)$  are the electron and hole densities determined from:

$$n(x) = N_c F_{1/2}(\eta_c) \quad (2)$$

and

$$p(x) = N_v F_{1/2}(\eta_v). \quad (3)$$

In the above equations,  $F_{1/2}$  and  $F_0$  are the Fermi Integral;  $\eta_c$  and  $\eta_v$  are the Plank potential for electron and hole.

The effective density of states in conduction band ( $N_c$ ) and the effective density of states in valence band ( $N_v$ ) for the bulk regions are:

$$N_{c,v}(x) = \frac{1}{4\pi^{3/2}} \left( \frac{2m_{n,p}^*(x)kT_{n,p}(x)}{\hbar^2} \right)^{3/2} \quad (4)$$

For the quantum well region the effective 2D density of states for conduction band ( $N_{cQW}$ ) and valence band ( $N_{vQW}$ ) are:

$$N_{c,vQW} = \frac{m_{n,p}^* kT_{n,p}}{\pi \hbar^2} \quad (5)$$

In the above equations,  $m_{n,p}^*$  are density of states masses for electron and hole;  $k$  and  $\hbar$  are the Boltzmann and Plank constants, respectively; and  $T_n$  is the electron temperature and  $T_p$  is the hole carrier temperature.

In the QW the quantized energy levels for electrons ( $E_{QWn}$ ) and holes ( $E_{QWp}$ ) are computed from an analytical expression assuming a finite square well approximation:

$$\sqrt{\frac{2m_{QWn,p}^* E_{QWn,p}}{\hbar^2}} \tan\left(\sqrt{\frac{2m_{QWn,p}^* E_{QWn,p}}{\hbar^2}} \frac{L_{QW}}{2}\right) - \sqrt{\frac{2m_{BULK n,p}^* (V_{QWn,p} - E_{QWn,p})}{\hbar^2}} = 0 \quad (6)$$

where  $m_{QWn,p}^*$  are the electron and hole density of state masses in a quantum well and  $m_{BULK n,p}^*$  are electron and hole density of state masses in the bulk material. In Eq. (6),  $V_{QWn}$  and  $V_{QWp}$  are conduction and valence heights in the QW, respectively, and  $L_{QW}$  is the well thickness. Both bound and free carriers are considered in the quantum well region.

A non-isothermal drift-diffusion current continuity equations for electron ( $J_n$ ) and hole carriers ( $J_p$ ) are considered:

$$\frac{1}{q} \nabla \cdot J_n(x) - (U_{SRH} + U_{b-b} - G_{OPT}) = 0 \quad (7)$$

$$\frac{1}{q} \nabla \cdot J_p(x) + (U_{SRH} + U_{b-b} - G_{OPT}) = 0 \quad (8)$$

where

$$J_n = \mu_n n$$

$$\left[ (kT_n \nabla \eta_c + \nabla E_c) + \left(\frac{\xi}{2} + \nu_n\right) \frac{F_{3/2+\nu_n}(\eta_c)}{F_{1/2+\nu_n}(\eta_c)} \nabla kT_n \right] \quad (9)$$

and

$$J_p = -\mu_p p$$

$$\left[ (kT_p \nabla \eta_v - \nabla E_v) + \left(\frac{\xi}{2} + \nu_p\right) \frac{F_{3/2+\nu_p}(\eta_v)}{F_{1/2+\nu_p}(\eta_v)} \nabla kT_p \right] \quad (10)$$

The constants  $\nu_n$  and  $\nu_p$  are the phonon scattering parameters [8]. In the above equations, the net generation/recombination terms are presented by band-to-band Auger recombination ( $U_{b-b}$ ):

$$U_{b-b} = B(np - n_i^2) \quad (11)$$

and Shockley-Read-Hall recombination ( $U_{SRH}$ ):

$$U_{SRH} = \frac{np - n_i^2}{(p + n_i)\tau_n + (n + n_i)\tau_p} \quad (12)$$

The optical generation term ( $G_{OPT}$ ) represents both the monochromatic single photon energy as well as solar spectrum [9].

For the simplicity of implementing the model, we have assumed that the transit time across the quantum well is zero so that the quantum well can be treated as a block in which the rate equations are not solved. Instead, the model uses the flux of carriers in and out of the quantum-well including generation-recombination terms in the well, where the bulk recombination terms are modified and extended to quantum well region:

$$U_{b-b} = \frac{1}{L_{QW}} \left| \int_0^{L_{QW}} \psi_n(x) \psi_p(x) dx \right|^2 B_{QW} (n_{2d} p_{2d} - n_{i,2d}^2) \quad (13)$$

and

$$U_{SRH} = \frac{1}{L_{QW}} \left| \int_0^{L_{QW}} \psi_n(x) \psi_p(x) dx \right|^2 \cdot \frac{(n_{2d} p_{2d} - n_{i,2d}^2)}{(p_{2d} + n_{i,2d})\tau_{n0} + (n_{2d} + n_{i,2d})\tau_{p0}} \quad (14)$$

where  $n_{2d}$  and  $p_{2d}$  are total QW electron and hole concentrations, given by:

$$n_{2d} = N_{cQW} F_0(\eta_c - \frac{E_{QWn}}{kT_n}) \quad (15)$$

$$p_{2d} = N_{vQW} F_0(\eta_v - \frac{E_{QWp}}{kT_p}) \quad (16)$$

In this model, the bound carriers in the well are calculated according to the probability distribution given by the wave functions,  $\psi_{n,p}$ . The computed separation of the confined and free carriers is used to determine the density of states for those carriers eligible for thermionic emission [10]. The thermionic emission model for heterostructure is applied to single quantum well device by including coefficient that considers such effects as the different effective masses, quantum mechanical

transmission into barrier, the quantum mechanical reflection at the interface.

In Eq.(12),  $n_i$  is the intrinsic carrier concentration in the bulk and in Eq. (13)-(14),  $n_{i,2d}$  is the intrinsic carrier concentration in the quantum well.

Based on the Stratton's energy-balance derivations for hot carriers, the kinetic flux density equations for electrons ( $S_n$ ) and holes ( $S_p$ ) are:

$$\nabla \cdot S_{n,p}(x) + W_{n,p}(x) = 0$$

(17)

and for the lattice is given by

$$\nabla \cdot S_L(x) - W_L(x) = 0$$

(18)

where

$$S_L(x) = -\kappa(x)\nabla T_L$$

(19)

$$S_n = -\mu_n n \frac{kT_n}{q} \left[ \left( kT_n \nabla \eta_c + \nabla E_c \right) \left( \frac{5}{2} + \nu_n \right) \frac{F_{3/2+\nu_n}(\eta_c)}{F_{1/2+\nu_n}(\eta_c)} + \nabla kT_n \left( \frac{7}{2} + \nu_n \right) \left( \frac{5}{2} + \nu_n \right) \frac{F_{5/2+\nu_n}(\eta_c)}{F_{1/2+\nu_n}(\eta_c)} \right] - \frac{E_c J_n}{q}$$

(20)

and

$$S_p = -\mu_p p \frac{kT_p}{q} \left[ \left( kT_p \nabla \eta_v - \nabla E_v \right) \left( \frac{5}{2} + \nu_p \right) \frac{F_{3/2+\nu_p}(\eta_v)}{F_{1/2+\nu_p}(\eta_v)} + \nabla kT_p \left( \frac{7}{2} + \nu_p \right) \left( \frac{5}{2} + \nu_p \right) \frac{F_{5/2+\nu_p}(\eta_v)}{F_{1/2+\nu_p}(\eta_v)} \right] - \frac{E_v J_p}{q}$$

(21)

In Eq. (17),  $W_n$  and  $W_p$  are the kinetic energy loss rate for electrons and holes (Joules per volume per second) which represent various kinetic energy exchanges among the carriers and lattice, and among the carriers themselves:

$$W_{n,p} = W_{n,p,SRH} + W_{n,p,b-b} + W_{n,p,RELAX} - W_{n,p,OPT}$$

(22)

In Eq. (18),  $W_L$  is the total energy exchange with lattice:

$$W_L = W_{n,SRH} + W_{p,SRH} + W_{n,RELAX} + W_{p,RELAX}$$

(23)

In Eq. (22), the carrier energy loss rates due to SRH and band-to-band mechanisms for electrons ( $n$ ) and holes ( $p$ ) are given by:

$$W_{n,SRH} = \left( \frac{u_n}{n} \right) U_{SRH}$$

(24)

$$W_{p,SRH} = \left( \frac{u_p}{p} \right) U_{SRH}$$

(25)

$$W_{n,b-b} = \left( \frac{u_n}{n} \right) U_{b-b}$$

(26)

$$W_{p,b-b} = \left( \frac{u_p}{p} \right) U_{b-b}$$

(27)

where the kinetic energy for electrons ( $u_n$ ) and holes ( $u_p$ ) at a given temperature is  $u_{n,p} = \frac{3}{2} k_B T_{n,p}$ , related by carrier temperature and carrier populations, modeled by the interaction of carrier and phonon lattice.

In Eq. (23), the kinetic energy exchange among the lattice and carriers are modeled by energy relaxation lifetime for electrons  $\tau_{n,E}$  and energy relaxation lifetime for holes  $\tau_{p,E}$  [9]:

$$W_{n,RELAX} = \frac{u_n(T_n) - u_n(T_L)}{\tau_{n,E}}$$

(28)

and

$$W_{p,RELAX} = \frac{u_p(T_p) - u_p(T_L)}{\tau_{p,E}},$$

(29)

where  $T_L$  is the lattice temperature and normally at room temperature.

The expression for the direct kinetic energy exchange among the electron and hole carriers based on the effective mass approximation due to optical generation for electron ( $W_{n,OPT}$ ) and holes ( $W_{p,OPT}$ ) in the bulk have the forms [10, 11]:

$$W_{n,OPT} = E_c G_{OPT} + \sum_{h\nu_{OPT}} \frac{m_p^*}{m_n^* + m_p^*} (h\nu_{OPT} - E_g)$$

$$G_{\nu_{OPT}} \quad (30)$$

and

$$W_{p,OPT} = -E_v G_{OPT} + \sum_{h\nu_{OPT}} \frac{m_n^*}{m_n^* + m_p^*} (h\nu_{OPT} - E_g)$$

$$G_{\nu_{OPT}} \quad (31)$$

Equations (30) and (31) are modified for the QW and have the forms:

$$W_{n,OPT} = +(E_{n,QW} + E_c) G_{OPT} + \sum_{h\nu_{OPT}} \frac{m_p^*}{m_n^* + m_p^*} (h\nu_{OPT} - E_{g,QW}) G_{\nu_{OPT}}$$

$$(32)$$

and

$$W_{p,OPT} = +(E_{p,QW} - E_v) G_{OPT} + \sum_{h\nu_{OPT}} \frac{m_n^*}{m_n^* + m_p^*} (h\nu_{OPT} - E_{g,QW}) G_{\nu_{OPT}},$$

$$(33)$$

where  $h\nu_{OPT}$  is the energy of the absorbed incident photon.

It is noted that according to the *Stratton's* energy-balance equations the flux density of electron kinetic energy and mean electron energy and electron temperature are strongly coupled [7]. The net kinetic energy loss rate for electrons (Joules per volume per second) represents various kinetic energy exchange among the carriers and lattice, and among the carriers themselves which is modeled by an average energy relaxation lifetime ( $\tau_E$ ). The release of energy by the carriers is modeled by the interaction of phonons and electrons and net energy loss rate due to *Shockley-Read-Hall* nonradiative mechanism and the loss of kinetic energy due to radiative recombination through emission of photons. These interactions causes the lattice to heat up. The resulting heat includes several sources such as Joules heat, generation-recombination heat, and *Thomson* and *Peltier* relationships [8, 9]. In the model implemented, we have assumed that hole carriers thermalize to the lattice temperature instantaneously. This assumption is valid as it is shown in the experimental work for determining the electron energy relaxation lifetime in  $Al_xGa_{1-x}As/GaAs$  QW *p-i-n* devices.

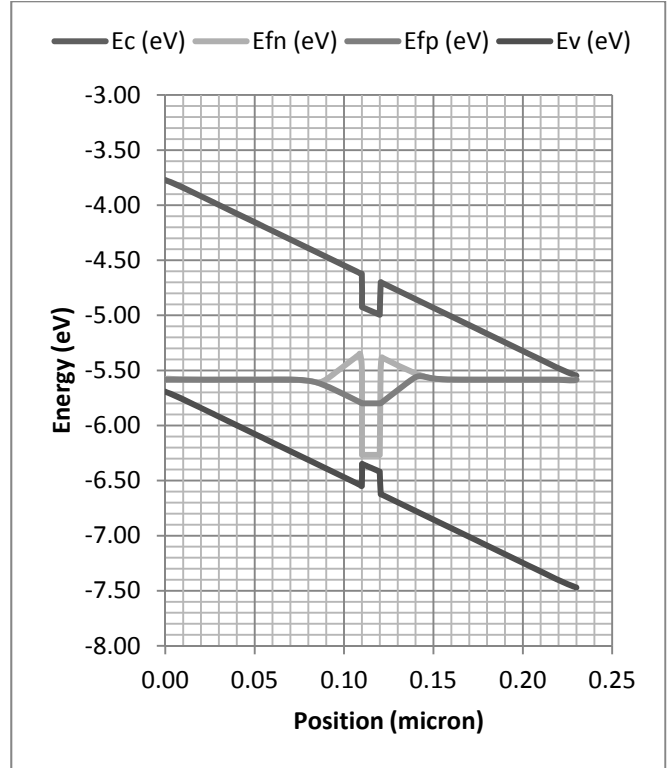


Figure 2. Band structure of a single quantum well  $Al_xGa_{1-x}As /GaAs$  cell. The multi quantum wells are treated as single QW's with no overlap and coupling effect.

### III. RESULTS AND DISCUSSIONS

A numerical simulation approach is employed to study the effects of carrier escape from quantum well and the interaction of hot electrons with crystal lattice in QW hot carrier solar cells where the cooling dynamics in photo-excited structures affect the cell efficiency. Simulation data show that hot carriers escape from multi quantum well results in a higher maximum conversion point in structures with long energy relaxation lifetime which may lead to a higher efficiency in hot electron solar cells. The band structure of an  $AlGaAs/GaAs$  single cell is shown in Figure 2. The QW is embedded in the center of the *p-i-n* diode. In detailed energy balance equations the non-isothermal current density is solved to determine the electron temperature. The electron temperature distribution for different energy relaxation lifetime is shown in Figure 3, where the energy transfer among the charge carriers and crystal lattice is modeled by an average energy relaxation lifetime. The temperature in the well is

constant due to quantized energy level of the well. The average electrons populations stay hot for a longer energy lifetime due to less of energy loss to the lattice. Figure 3 shows that in a multiquantum well structure hot electrons with longer energy relaxation time tend to stay at higher energy before relaxing to the lattice.

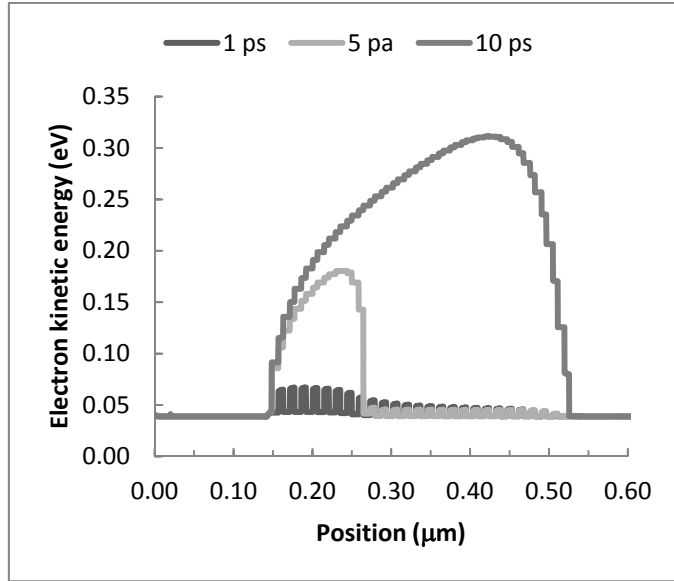


Figure 3. In a multiquantum well structure hot electrons with longer energy relaxation time tend to stay at higher energy before relaxing to the lattice.

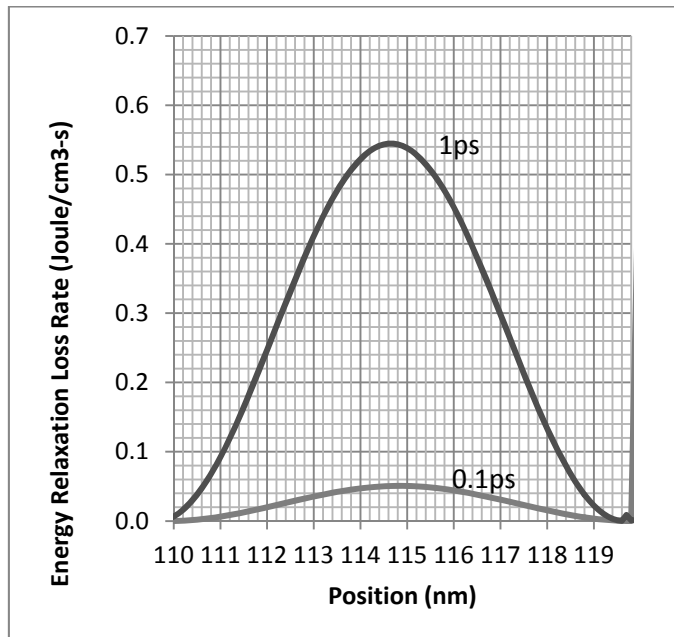


Figure 4. The Energy relaxation loss rate for

different relaxation energy lifetime.

The net energy loss rate for a single *QW* p-i-n diode is shown in Figure 4. In addition to this rate, the limiting *Shockley-Read-Hall* recombination rate per unit volume is also considered. The result of simulation for the single *QW* p-i-n diode showing *Shockley-Read-Hall* recombination energy rate at different energy lifetime is shown in Figure 5. This loss rate is higher for samples with longer energy lifetime since this parameter controls the average population of the electrons in the *QW*. The result of simulation for electron distribution at different energy relaxation lifetime is shown in Figure 6. A higher carrier density in the well translates to a higher *SRH* energy loss rate.

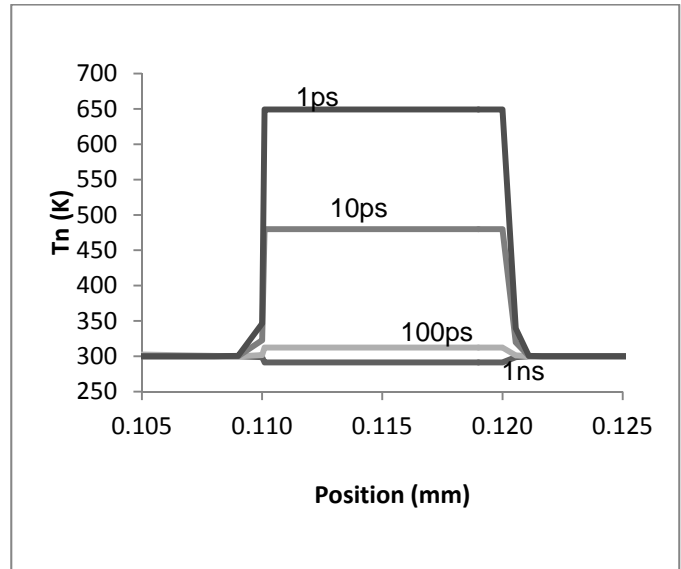


Figure 5. SRH energy loss rate in the QW for different carrier lifetimes. Both free and bulk SRH rates are considered in the model.

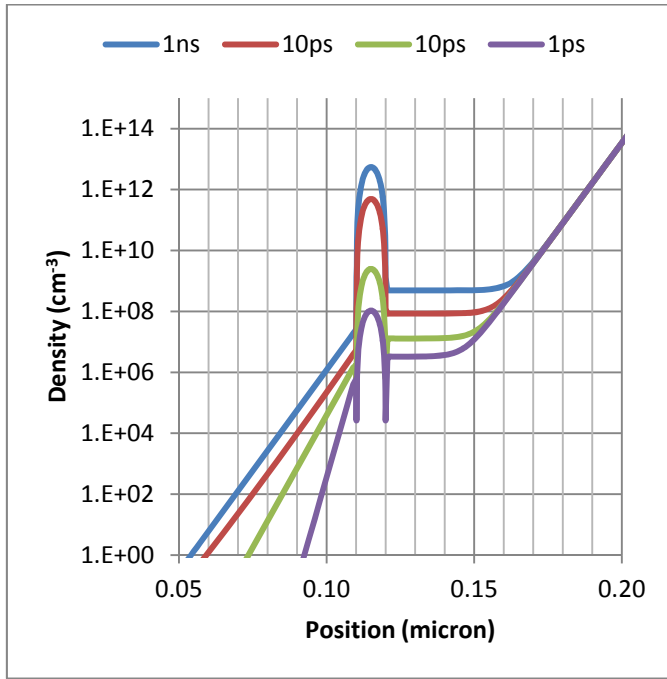


Figure 6. The simulated result for electron concentration in QW by increasing energy relaxation lifetime from 1ps to 1ns. The figure on the right shows the zoomed section in QW region of the p-i-n diode.

We have studied an  $Al_xGa_{1-x}As$  /  $GaAs$  structure with several quantum wells placed in the intrinsic region similar to the device described in reference [5]. The quantum wells are modeled with  $60 \text{ \AA}$   $Al_xGa_{1-x}As$  barriers and  $85 \text{ \AA}$   $GaAs$  wells and the  $Al$  composition is  $x=0.35$ . The  $p$ -type and  $n$ -type layers are also made out of the barrier  $Al_xGa_{1-x}As$  material. Parameters used in the simulation are taken from published literature summarized in Table I. The numerical model presented in this work is aimed at improving the existing device models for the characterization of nano-structure hot carrier solar cells.

TABLE I

DEVICE PARAMETERS USED IN 30 QW  $Al_xGa_{1-x}As$  /  $GaAs$   
HOT ELECTRON SOLAR CELL

Parameters	Value
$p^+$ $GaAs$ cap thickness	$0.02 \text{ \AA m}$
$p^+$ $GaAs$ cap doping	$1.8 \times 10^{18} \text{ cm}^{-3}$

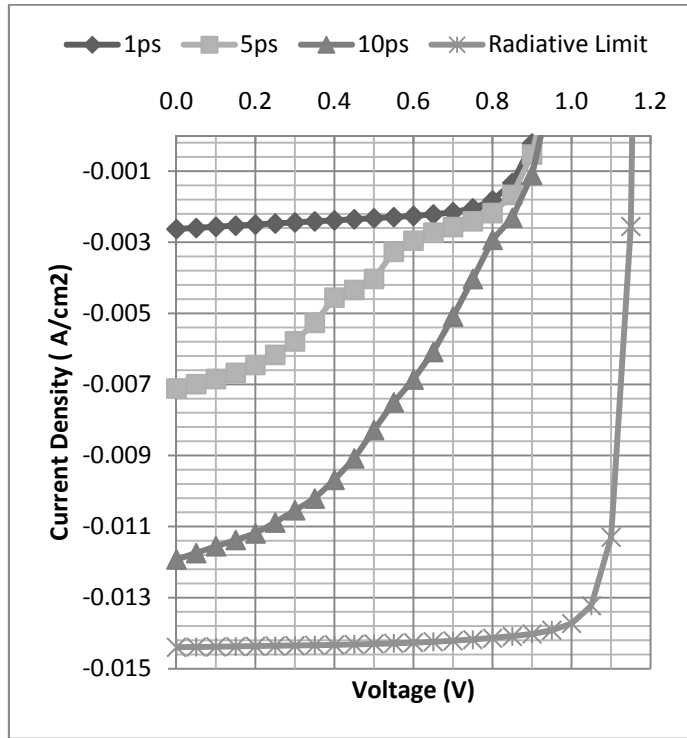
$p$ layer $Al_xGa_{1-x}As$ thickness	$0.3 \text{ \AA m}$
$p$ layer $Al_xGa_{1-x}As$ doping	$7 \times 10^{17} \text{ cm}^{-3}$
$i$ - region thickness	$0.48 \text{ \AA m}$
$n$ layer $Al_xGa_{1-x}As$ thickness	$0.3 \text{ \AA m}$
$n$ layer $Al_xGa_{1-x}As$ doping	$7 \times 10^{17} \text{ cm}^{-3}$
Quantum well's ( $GaAs$ ) thickness	$85 \text{ \AA}$
Quantum barrier's ( $Al_xGa_{1-x}As$ ) thickness	$60 \text{ \AA}$
$Al$ composition material, $x$	$0.2-0.46$
SRH lifetime	$1-30 \text{ ns}$
Surface recombination velocity ( $S_n, S_p$ )	$1 \times 10^5 \text{ cm/s}$
Energy relaxation lifetime ( $\tau_E$ )	$1-10 \text{ ps}$

Multi quantum well structures can slow down the cooling process (carriers with long energy relaxation lifetime) by reducing the phonon scattering effects. In this process, the rate at which the carriers are lost to the lattice is slowed down so called carriers escape. As a result, quantum well theoretically can enhance solar cell efficiency in devices by reducing the non-radiative recombination effect.

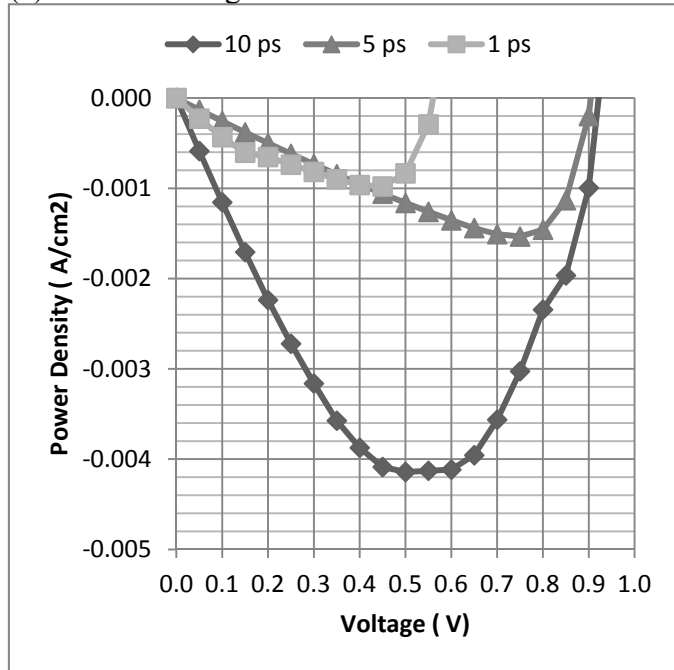
Figure 7(a) shows the simulated current-voltage characteristics of QW photodiode with 30 periods for three different values of energy relaxation lifetime, computed in an air mass 1.5 spectrum. These results show that hot electron effects lead to an increase in short circuit current. The increase in short circuit current is due to hot carriers escaping from the wells without any significant SRH recombination. As shown in Figure 7(b), the maximum power point is higher in a device with longer energy lifetime. Long energy relaxation lifetime slows the cooling dynamics and increases the rate of carriers escaping from the quantum

wells, which may lead to a higher cell efficiency. These results support the experimental data recently published by others [2, 5].

Current-voltage characteristics, (b) Conversion power output.



(a) Current-voltage characteristics



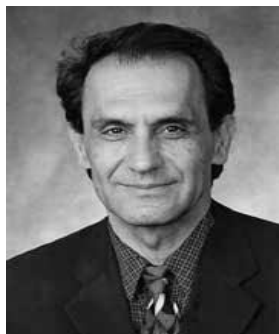
(b) Conversion power output

Figure7. A 30 QW  $Al_{0.35}Ga_{0.65}As/GaAs$  p-i-n diode simulated in an air mass1.5 spectrum with an energy relaxation lifetime of  $\tau_E = 1, 5,$  and  $10$  ps, (a)

#### REFERENCES

- [1] Sze, S. M. *Modern Semiconductor Device Physics*. New York: Wiley, 1998. Print.
- [2] M. D. Kelzenberg et al., "Photovoltaic measurements in single-nanowire Silicon Solar cells," *Nano Lett.*, no. 2, pp. 710-714, 2008.
- [3] T. J. Kempa, B. Tian, D. R. Kim, J. Hu, X. Zheng, and C. M. Leiber, "Single and Tandem Axial p-i-n nanowire Photovoltaic Devices," *Nano Lett.*, no. 10, pp. 3456-3460, 2008.
- [4] R. Corkish and C. B. Honsberg, "Dark currents in double-heterostructure and quantum-well solar cells," *26th IEEE Photovoltaic Specialist Conf.*, 1997.
- [5] J.G.J. Adams, W. Elder, G.Hill, J. S. Roberts, K.W.J. Barnham and N.J. Ekins-Daukes, Higher Limiting Efficiencies for Nanostructured Solar Cells, *Proc. of SPIE* Vol. 7597 759705-4, 2010.
- [6] K. Barnham et al., "Quantum well solar cells," *Applied Surface Science* 113/114, 722-733, 1997.
- [7] Urs Aeberhard, Microscopic Theory and Numerical Simulation of Quantum Well Solar Cells, *Proc. of SPIE* Vol. 7597 759702-11, 2010.
- [8] R. Stratton, "Semiconductor Current-Flow Equations (Diffusion and Degeneracy)", *IEEE Trans. on Electron Devices*, vol. ED-19, pp. 1288-1292, 1972.
- [9] D. Chen, Z. Yu, K.C. Wu, R. Goossens, R. Dutton, "Dual energy transport model with coupled lattice and carrier temperatures," *Proc. SISDEP V*, pp. 125-128, 1993.
- [10] Nelson, J. et al (1997), "Observation of suppressed radiative recombination in single quantum well p-i-n photodiodes," *Journal of applied physics*, vol. 82 no. 12, Dec. 15.
- [11] Song, G. H. (1991), Two-dimensional simulation of quantum-well lasers including energy transport, Technical Report CE-91-01, University of Illinois.
- [12] G. K. Wachutka, "Rigorous Thermodynamic Treatment of Heat generation and Conduction in Semiconductor Modeling," *IEEE Trans. On CAD*, vol. CAD-9, pp. 1141-1149. 1990.
- [13] Fardi, H., Numerical Modeling of Hot Electron  $GaAs/Al_xGa_{1-x}As$  Quantum Well Photovoltaics, *Proceedings of 35th IEEE Photovoltaic specialist Conference*, pp. 001800-00183, 2010.





**Hamid Fardi** received his PhD degree in Electrical Engineering from the University of Colorado at Boulder in 1986. He has been with the Department of Electrical Engineering of the University of Colorado Denver since 1992 where he is now a full professor. Before joining the UCD EE Department, he was a postdoctoral fellow at Rensselaer Polytechnic Institute, Troy, New York, in 1987. From 1988 to 1992, he was with NSF sponsored Millimeter-Microwave Computer Aided Design research center of the University of Colorado. In 1996 and 1997 he was a visiting research fellow at National Renewable Energy Lab (NREL). He currently holds a research affiliate position at National Institute of Standards and Technology (NIST), Boulder, Colorado, USA.

Dr Fardi consults with local and national semiconductor industry on device modeling and simulation of solid state electronics. His research interests concern the physics, design and modeling, and fabrication novel semiconductor devices. He has more than 100 publications in national and international archival journals and conference proceedings.

Dr. Fardi is a senior member of the IEEE and the faculty advisor for the IEEE Student Chapter at the University of Colorado Denver where he teaches undergraduate and graduate courses in electronics, solid state devices, and VLSI circuit simulation.